CHAPTER XXV-2

THE PERMANENT "VIRTUAL DENTITION"

Priscilla BAYLE, Arnaud MAZURIER & Roberto MACCHIARELLI

Abstract

Following the recent attribution of some newly identified fossil remains from the Betche aux Rotches cave near Spy, in Belgium, to the two adult Neandertal individuals Spy I and Spy II (Rougier et al.*, this volume: chapter XIX), the dentition of Spy I currently consists of 13 maxillary and 10 mandibular teeth (*in situ *or isolated), while that of Spy II of 10 maxillary and 16 mandibular teeth, mostly* in situ*. By using high-resolution microtomographic techniques, we have imaged the internal morphology of a whole sample of 28 permanent teeth selected from the two Neandertals and quantified their tissue proportions.*

The results fit the general patterns reported for the deciduous and permanent Neandertal teeth. Notably, compared to modern figures, both anterior and posterior teeth of Spy I and Spy II are characterised by similar absolute enamel volumes, but deposited over a topographically more complex enamel-dentine junction surface and larger volumes of dentine, finally resulting in lower average and relative enamel thickness values.

The present tooth by tooth analysis also reveals some differences in dental tissue proportions between the two Belgian fossil individuals. Compared to Spy I and to the adult Neandertal from Regourdou, the Spy II mandibular dentition shows a heterogeneous pattern of antero-posterior distribution of occlusal wear and dental tissue proportions.

INTRODUCTION

The reassessment of the odontoskeletal remains collected from the cave of Betche aux Rotches, near Spy, in Belgium (Fraipont & Lohest, 1886, 1887), has led to the identification of new human specimens, including dental material (Rougier *et al.*, 2004; Semal *et al.*, 2005, 2009). Some of the newly discovered teeth have been unequivocally associated to each of the two adult Neandertal skeletons, Spy I and Spy II, whose dentitions currently consist of 13 maxillary and 10 mandibular, and 10 maxillary and 16 mandibular permanent teeth, respectively (Rougier *et al.*, this volume: chapter XIX).

Recent advances in the fields of developmental biology, quantitative genetics, structural and comparative microanatomy show that a rich and varied amount of information is preserved at different levels in the dental tissues, which has fostered new research perspectives in palaeoanthropology (Wood, 2010). However, a significant portion of this record, which is crucial for assessing the evolutionary pathways and phylogenetic relationships, as well as the adaptive strategies and fluctuating variation patterns of extant and extinct taxa, is hidden at the meso-microstructural level, and lies imprinted deeply inside the crown and the roots (Macchiarelli & Bailey, 2007).

The increasing use in palaeobiology and palaeoanthropology of microtomographic (μCT) techniques capable to virtually explore, to extract, and to render, in a 2-3D perspective at varied resolutions, a number of subtle details of the internal structure of dental tissues has recently provided new evidence to the understanding of the Neandertal dentition. More precisely, compared to the modern human figures, both deciduous and permanent Neandertal teeth are characterised by similar absolute enamel volumes, but deposited over a topographically more complex enamel-dentine junction surface and larger volumes of dentine, thus resulting in lower average and relative enamel thickness values (e.g. Macchiarelli *et al.*, 2006; Olejniczak *et al.*, 2008; Skinner *et al.*, 2008; Bayle *et al.*, 2009; Toussaint *et al.*, 2010).

However, only a negligible number of complete Neandertal dentitions have been described so far for their inner structural features,

and extremely poor quantitative information is still available on dental tissue proportions of anterior teeth and premolars (Smith *et al.*, 2007; Macchiarelli *et al.*, 2008; Bayle *et al.*, 2009; Crevecoeur *et al.*, 2010; Bayle & Macchiarelli, this volume: chapter XX-3). Conversely, the comparative characterisation of the internal morphology and tissue proportions of the elements of the anterior dental arch may bring new evidence to test the traditional suggestions, mostly relying on observations derived from their absolutely and relatively large dimensions and high degree of occlusal wear, that in Neandertals these teeth may have been specifically adapted to face more frequent and/or heavier masticatory and/or paramasticatory loadings (e.g. Brace, 1964; Wolpoff, 1979; Trinkaus, 1983; O'Connor *et al.*, 2005).

Here, we report the results of the microtomographic-based 3D "virtual" investigation and quantitative characterisation of the inner morphology of a whole of 28 selected maxillary and mandibular teeth from the two Neandertal skeletons Spy I and II. More specifically, dental tissue proportions have been assessed in these two adults and then compared to the evidence from other Neandertal specimens, including the complete mandibular dentition of the Regourdou 1 individual, in France (Macchiarelli *et al.*, 2008), as well as to the modern human figures reported so far. Also, in the case of Spy II's complete mandibular dentition, the degree of symmetry of its endostructural features, which is still unreported for any Neandertal dentition, has been quantified.

METHODS

The structural morphology of the 28 selected teeth representing the two individuals Spy I and Spy II (Table 1) has been investigated

Spy I							
Maxillary teeth				*Mandibular teeth*			
Left		*Right*		*Left*		*Right*	
I1			*I1*	*I1*	Spy 571a•		*I1*
I2	Spy 11I		*I2*	*I2*			*I2*
C		Spy 11G	*C*	*C*			*C*
P3	Spy 11F		*P3*	*P3*			*P3*
P4	Spy 11E		*P4*	*P4*	Spy 11H		*P4*
M1	Spy 11C		*M1*	*M1*			*M1*
M2	Spy 11D		*M2*	*M2*			*M2*
M3	Spy 583a (on Spy 11B)	Spy 94a	*M3*	*M3*			*M3*

Spy II							
Maxillary teeth				*Mandibular teeth (on Spy 3)*			
Left		*Right*		*Left*		*Right*	
I1	Spy 92b		*I1*	*I1*	Spy 577b	Spy 577a	*I1*
I2			*I2*	*I2*	Spy 577d	Spy 577c	*I2*
C			*C*	*C*	Spy 577f	Spy 577e	*C*
P3			*P3*	*P3*	Spy 577h	Spy 577g	*P3*
P4			*P4*	*P4*	Spy 577j	Spy 577i	*P4*
M1			*M1*	*M1*	Spy 577l	Spy 577k	*M1*
M2			*M2*	*M2*	Spy 577n	Spy 577m	*M2*
M3		Spy 578f (on Spy 2A)	*M3*	*M3*	Spy 577p	Spy 577o	*M3*

•: The position of the lower incisor Spy 571a is uncertain (see Maureille *et al.*, this volume: chapter XXV-1).

Table 1. The 28 permanent teeth of the Neandertal adult individuals Spy I and Spy II investigated for dental tissue proportions in the present microtomographic-based analysis.

using a high-resolution µCT record. The mandible Spy 3, which belongs to the individual Spy II and bears a complete dentition, was imaged at the *Centre de Microtomographie* set at the University of Poitiers, France (equipment X8050-16 Viscom AG; camera 1004 × 1004), while the other 12 teeth from both Spy I and Spy II, isolated or not, were detailed at the Micro CT Scan Research Group laboratory of the University of Antwerp, Belgium (equipment Skyscan 1076 *in vivo* X-ray microtomograph).

Scans of Spy 3 were performed at 130 kV, 175 µA current, 16 integrations/projection, and a projection each 0.2°. The final volumes were reconstructed using DigiCT v.2.3.3 (Digisens), with an isotropic voxel size of 67.61 μm^3 for the left hemi-mandible, and of 64.31 μm^3 for the right one. For the other dental specimens, scan parameters were as follows: 100 kV, 100 µA current, between 12 and 16 integrations/projection, and a projection each 0.5-0.7°. The final volumes were reconstructed using NRecon v.1.3 (Skyscan), with an isotropic voxel size of 17.69 μm^3. In order to facilitate their numerical processing, the original resolution of these volumes was halved, leading to a voxel size of 35.38 μm^3.

In all cases, a semi-automatic threshold-based segmentation with manual corrections was carried out by using AMIRA v.5.2 (Visualisation Sciences Group) and Artecore v.1.0 (NESPOS Society). Threshold values between segmented components (air, bone, dentine, enamel, and sediment) were found according to the methodology of Spoor *et al.* (1993). However, thanks to their rather good preservation quality and modest degree of mineralisation and diagenetic change, no particular technical difficulties were encountered in segmenting the entire sample of 28 selected teeth. The crowns were digitally isolated from the roots and surface rendering was performed using triangulation and constrained smoothing from the volumetric data (Olejniczak *et al.*, 2008).

For the purposes of the present study, the following nine linear, surface, and volumetric variables describing tooth tissue proportions have been digitally measured or calculated: the volume of the enamel cap (mm^3); the volume of the dentine (mm^3); the volume of the pulp (mm^3); the total tooth volume (mm^3); the volume of the crown dentine+pulp (mm^3); the surface area of the enamel-dentine junction (EDJ; mm^2); the percent of the crown volume that is dentine and pulp; the Average Enamel Thickness (AET; mm); and the scale-free Relative Enamel Thickness (RET) (methodological details in Kono, 2004; Macchiarelli *et al.*, 2006; Olejniczak *et al.*, 2008). AET is the average straight-line distance between the EDJ and the outer enamel surface, calculated as the quotient of the enamel volume and EDJ surface area; RET is the AET scaled by the cube root of the crown dentine+pulp volume and multiplied by 100 (Martin, 1985; see also Olejniczak *et al.*, 2008).

Group	*Site/sample*	*Age*	*UM3*	*LM3*	*Total*
Neandertal	Abri Suard	MIS 6		2	2
	Abri Bourgeois-Delaunay	MIS 5e		1	1
	Krapina	MIS 5e		1	1
	Regourdou	MIS 5-4		2	2
	El Sidrón	MIS 3	3		3
	La Quina	MIS 3		1	1
	Le Moustier	MIS 3	1	1	2
	Spy	MIS 3	3	2	5
Extant	EH	Present	15	10	25

Table 2. Composition of the Neandertal and extant human comparative dental samples used for the upper (UM3) and lower third molars (LM3). Origin, reference group, age (marine isotope stage), and tooth-specific sample size of the microtomographic-based dental sample are provided. Data sources: Kono (2004), Macchiarelli *et al.* (2006, 2008), Olejniczak *et al.* (2008), and original data.

The 3D topographic mapping of the site-specific enamel thickness variation (*cf.* Macchiarelli *et al.*, 2008; Bayle *et al.*, 2010) was realised from the segmented enamel and crown dentine components and rendered using a chromatic scale, where thickness increases from dark blue up to red.

For the upper M3s, the lower incisors, and the lower P4s of Spy I and Spy II, the results of the analysis of the tooth crown and root components have been directly compared between these two individuals, while those relative to the complete Spy II's lower dentition have been distinctly compared to the microtomographic-based evidence from the mandibles of a young adult extant human of European origin (virtually unworn crowns) and the Regourdou 1 Neandertal skeleton (Macchiarelli *et al.*, 2008). Also, for the enamel and crown dentine+pulp volumes, the EDJ surface area, the percent of the crown volume that is dentine and pulp, the AET and RET, the results from the analysis of the relatively modestly worn upper and lower M3s of both Belgian fossil individuals have been compared to the virtual record from a sample of 12 Neandertal teeth (including four upper M3s and eight lower M3s) selected from the sites of Abri Suard, Abri Bourgeois-Delaunay, Regourdou, La Quina, and Le Moustier, in France, Krapina, in Croatia, El Sidrón, in Spain, as well as to a worldwide extant human dental reference sample (EH) consisting of 25 teeth (15 upper M3s and 10 lower M3s; original data from Kono, 2004; Macchiarelli *et al.*, 2006, 2008; Olejniczak *et al.*, 2008) (Table 2).

RESULTS AND DISCUSSION

The reconstructed complete mandibular dentition of Spy II is shown in Figure 1. In order to assess tissue proportions, each tooth has been virtually extracted from its socket and, as occurred for the entire dental set representing Spy I and Spy II, the tooth components (enamel, dentine, and pulp cavity) have been isolated and rendered in different colours (Figure 1). With the only three exceptions of an apical break affecting the lingual root of the upper left M1, in Spy I (see Figure 2), an enamel loss at the buccal aspect of the lower right P3, in Spy II (*ca.* 16 % of the enamel volume lost compared to the antimere), and a slight apical break at the mesial root of the lower right M2, again in Spy II (*ca.* 4 % of the total dentine volume lost compared to the antimere), all remaining examined teeth from both individuals are quite well preserved.

The virtual reconstructions of the outer enamel surface (OES) in semi-transparency and of the EDJ of the Spy I upper left M1 and M2 and Spy II lower molars are shown in Figure 2. Because of dental wear, the OES morphology of the M1s and M2s is hardly appreciable.

In Spy I, the rendering of the EDJ surfaces reveals the presence of a Carabelli's trait on the mesio-lingual aspect of the upper left M1 and M2, while in Spy II a trigonid crest is found in all lower molars (Figure 2). The latter trait, which

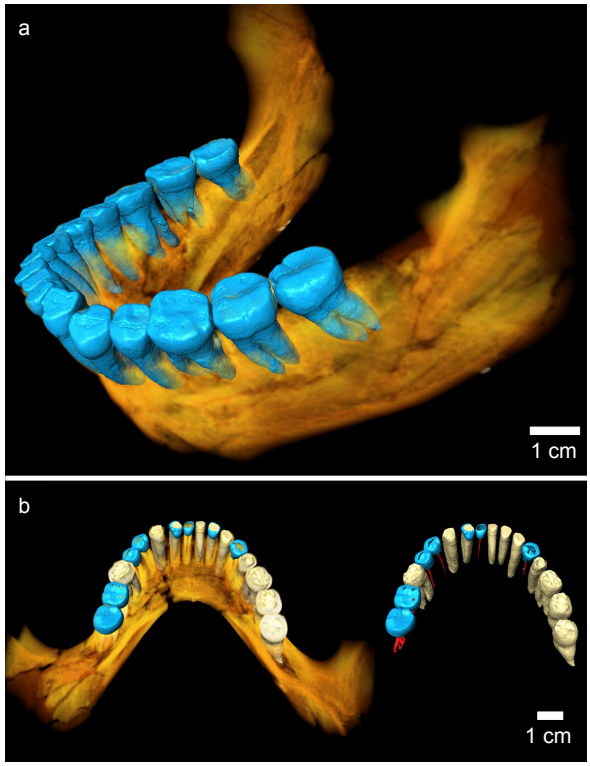

Figure 1. a: Microtomographic-based 3D reconstruction in lateral oblique view (volume rendered in transparency) of the Spy II mandible (specimen Spy 3; see Table 1) bearing a complete permanent dentition; b: randomly selected examples of virtually extracted dental components in occlusal view (enamel, dentine, and pulp cavity) shown in different colours.

is defined at the EDJ surface during early tooth germ development (Macchiarelli *et al.*, 2008; Skinner *et al.*, 2008), shows a significantly higher occurrence in Neandertal than in recent/modern human lower molars (e.g. Bailey, 2002; Bailey *et al.*, 2011).

For each investigated tooth selected from Spy I and Spy II, dental tissue proportions are shown in Table 3 (maxillary teeth) and in Table 4 (mandibular teeth), the latter also presenting the results gathered from the analysis of the mandibular dentition of an extant young adult individual used here as comparative reference (EH; right side only).

For the same tooth types available for direct comparison between Spy I and II − notably, the upper M3 and the lower incisors and P4 − all absolute variables (enamel, dentine, pulp, total tooth, crown dentine+pulp volumes, and EDJ surface area) and the percent of the crown

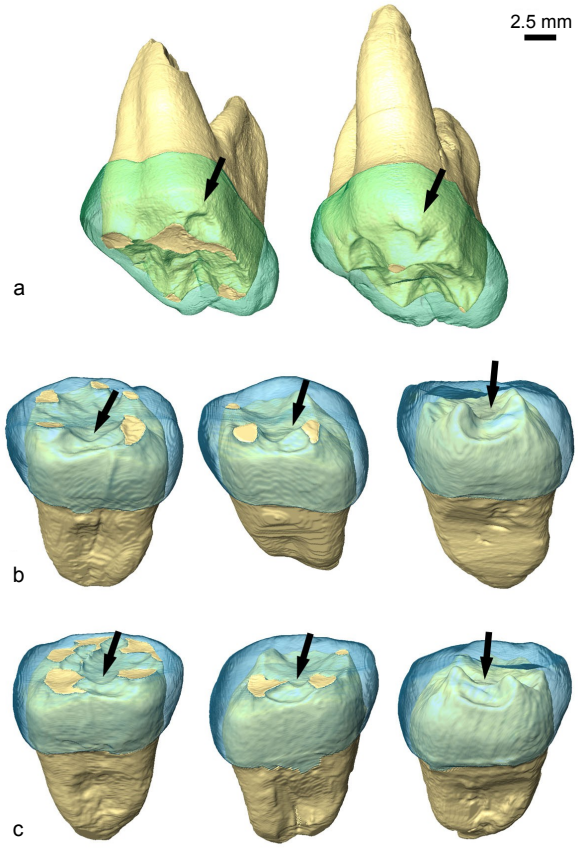

Figure 2. 3D virtual reconstruction of the upper left M1 (a, to the left) and M2 (a, to the right) of Spy I, and of the left (b; from left to right: M1 to M3) and right (c; from left to right: M1 to M3) lower molars of Spy II. The outer enamel surface (OES) is shown in semi-transparency and the arrows indicate the Carabelli’s traits (a) and the trigonid crests (b, c) detectable at the level of the enamel-dentine junction (EDJ) surface. Teeth shown in occluso-mesial view and dental tissues rendered in different colours.

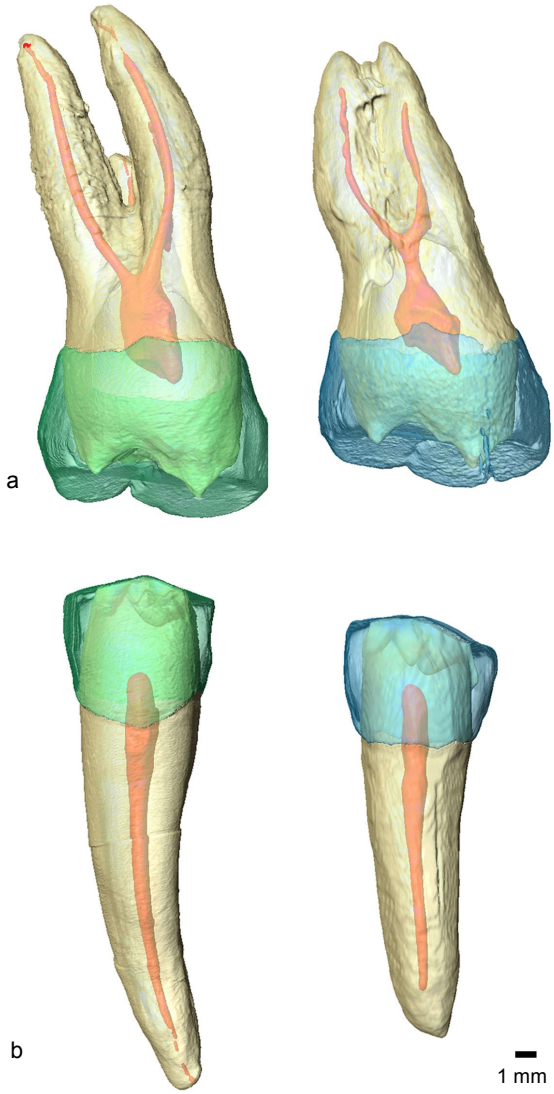

Figure 3. Comparative 3D virtual reconstruction of the same tooth types examined in Spy I (to the left) and Spy II (to the right). a: upper right M3s; b: lower left P4s. Teeth shown in buccal view. The volumes of the virtually reconstructed teeth are rendered in transparency and each tooth component (enamel, dentine, and pulp cavity) is shown in a different colour.

volume that is dentine and pulp, show slightly higher values in Spy I. Despite a modest difference between antimeres recorded in Spy II for the endostructural signals from the lower incisors and P4s (see Table 4), AET and RET are generally higher in this individual than in Spy I (e.g. RET mean value of 16.36 for the upper M3s in Spy I *vs*. 18.43 in Spy II; Table 3). Even if the results from the analysis of the incisors and, to a lesser extent, of the premolars, are affected by advanced occlusal wear (which, in the case of the incisors, also affects the dentine), the evidence from the upper M3s points to a certain level of variation between the two Neandertal individuals. Notably, compared to Spy II, Spy I has bigger teeth with larger dentine and pulp volumes and slightly thinner enamel (Figure 3).

As shown in Table 4, the average and relative enamel thickness values are lower in Spy II than in the modern human individual used in the present study for all mandibular tooth types, while the estimates for the dentine, pulp, total tooth volumes, and the percent of the crown volume that is dentine and pulp are higher in the Neandertal individual. Compared to the modern human reference dentition, higher values are found in Spy II's postcanine teeth for the crown dentine+pulp volume and the EDJ surface area, but the opposite is true for the incisors and the canines. In this case, because of the degree of occlusal wear typically characterising the anterior dental arch of the fossil specimen, the modern estimates systematically exceed the Neandertal ones. As a whole, the enamel of the Spy II dentition is extensively affected by occlusal wear, but in this case the comparative volumetric values from the lower M3s suggest a certain degree of similarity between the Neandertal and the modern figures. It is also noteworthy

Maxillae	*Enamel volume (mm^3)*	*Dentine volume (mm^3)*	*Pulp volume (mm^3)*	*Total tooth volume (mm^3)*	*Crown dentine+pulp volume (mm^3)*	*EDJ surface area (mm^2)*	*% of the crown volume that is dentine+pulp*	*Average Enamel Thickness (mm)*	*Relative Enamel Thickness*
I1									
Spy II left	22.66*	536.12*	29.11	587.88*	89.06*	56.11*	80*	0.40*	9.04*
I2									
Spy I left	66.45*	657.92*	30.57	754.93*	140.15*	110.05*	68*	0.60*	11.62*
C									
Spy I right	77.08*	867.78*	41.11	985.97*	175.41*	115.91*	69*	0.67*	11.88*
P3									
Spy I left	141.11*	769.12	25.99	936.22	210.67	155.59	60*	0.91*	15.24*
P4									
Spy I left	141.79	753.24	24.86	919.90	185.85	147.23	57	0.96	16.88
M1									
Spy I left	189.87*	1,158.40	60.66	1,408.93	388.69	232.05	67*	0.82*	11.21*
M2									
Spy I left	247.87	1,350.37	58.16	1,656.40	418.51	250.31	63	0.99	13.24
M3									
Spy I left	213.84	1,019.74	46.46	1,280.04	280.72	199.32	57	1.07	16.38
Spy I right	224.48	1,035.58	50.08	1,310.13	301.55	205.05	57	1.09	16.33
Spy II right	198.60	755.58	34.83	989.01	233.73	174.95	54	1.14	18.43

*: Affected by occlusal wear.

Table 3. Linear, surface, and volumetric variables and dental tissue proportions virtually assessed on the 10 selected maxillary teeth of Spy I and Spy II. See text (Methods) for the description of the variables.

Mandibles	*Enamel volume (mm^3)*	*Dentine volume (mm^3)*	*Pulp volume (mm^3)*	*Total tooth volume (mm^3)*	*Crown dentine+pulp volume (mm^3)*	*EDJ surface area (mm^2)*	*% of the crown volume that is dentine+pulp*	*Average Enamel Thickness (mm)*	*Relative Enamel Thickness*
I1									
Spy I left•	29.77*	406.51*	17.73	454.02*	82.83*	78.65*	74*	0.38*	8.68*
Spy II left	12.68*	277.22*	12.68	302.57*	27.04*	32.13*	68*	0.39*	13.15*
Spy II right	7.14*	282.39*	10.81	300.34*	21.23*	21.93*	75*	0.33*	11.75*
EH	41.74	133.71	5.22	180.67	51.27	83.82	55	0.50	13.41
I2									
Spy I left•	29.77*	406.51*	17.73	454.02*	82.83*	78.65*	74*	0.38*	8.68*
Spy II left	18.91*	339.08*	10.18	368.17*	38.78*	42.10*	67*	0.45*	13.27*
Spy II right	12.64*	330.07*	11.85	354.56*	37.38*	37.17*	75*	0.34*	10.17*
EH	48.01	150.83	5.08	203.92	48.11	78.03	50	0.62	16.92
C									
Spy II left	40.87*	505.95*	13.37	560.19*	83.02*	66.39*	67*	0.62*	14.11*
Spy II right	34.47*	463.08*	12.16	509.71*	79.02*	64.83*	70*	0.53*	12.39*
EH	68.00	278.27	13.65	359.92	93.12	101.05	58	0.67	14.85
P3									
Spy II left	87.71*	415.76	14.43	517.90	117.47	100.59	57*	0.87*	17.80*
Spy II right	73.80*	386.57	11.74	472.11	119.94	90.82	62*	0.81*	16.48*
EH	104.63	246.82	11.23	362.67	89.52	98.11	46	1.07	23.84
P4									
Spy I left	123.38*	620.42	27.53	771.34	176.26	137.93	59*	0.89*	15.95*
Spy II left	106.30*	390.23	13.69	510.22	111.35	106.47	51*	1.00*	20.75*
Spy II right	92.32*	376.03	15.98	484.33	121.34	109.49	57*	0.84*	17.03*
EH	110.52	217.74	9.25	337.52	78.20	86.64	41	1.28	29.83
M1									
Spy II left	146.17*	719.69	42.29	908.15	260.97	176.90	64*	0.83*	12.93*
Spy II right	115.98*	766.74	30.00	912.71	251.77	162.97	68*	0.71*	11.27*
EH	203.32	579.58	34.78	817.68	255.07	186.55	56	1.09	17.19
M2									
Spy II left	181.50*	780.26	30.83	992.58	243.83	175.60	57*	1.03*	16.54*
Spy II right	168.84*	749.63	41.46	959.93	258.84	178.99	61*	0.94*	14.80*
EH	200.44	492.30	28.99	721.72	195.30	156.52	49	1.28	22.07
M3									
Spy II left	237.44	731.18	45.11	1,013.74	261.05	184.38	52	1.29	20.15
Spy II right	209.45	702.46	38.75	950.66	253.74	177.65	55	1.18	18.62
EH	203.13	438.56	27.62	669.30	161.76	144.46	44	1.41	25.81

•: The position of the lower incisor Spy 571a is uncertain (see Maureille *et al.*, this volume: chapter XXV-1).
*: Affected by occlusal wear.

Table 4. Linear, surface, and volumetric variables and dental tissue proportions virtually assessed on the 18 selected mandibular teeth of Spy I and Spy II, compared to the values from a young adult extant human specimen (EH; right teeth only). See text (Methods) for the description of the variables.

that the lower incisor and P4 of Spy I show a pattern similar to that displayed by the Spy II's postcanine teeth, i.e. similar enamel volumes to the modern individual but deposited over a larger volume of dentine, thus resulting in lower AET and RET values.

As mentioned above, for the first time in the case of a fossil specimen, the complete mandibular dentition of Spy II has been systematically investigated for its degree of structural symmetry. The results of this analysis are summarised in Table 4.

While the dentine, pulp, and total tooth volumes show no clear side dominance but only fluctuating asymmetry, the enamel, crown dentine+pulp volumes, EDJ surface area, and average and relative enamel thicknesses are systematically higher in the elements of the left hemi-arcade; conversely, the values of the percent of the crown volume that is dentine and pulp are systematically higher in the teeth from the right side. These differences are particularly marked in the case of the incisors, where the enamel volumes recorded for the left crowns are over 1.5 times higher (Table 4).

As noted, the results from the mandibular dentition of Spy II clearly reflect the higher degree of wear affecting the crowns of its right side (Maureille *et al.*, this volume: chapter XXV-1), which points to a preferential chewing side characterising this individual, likely related to a lateral asymmetry in the distribution of the bite forces (e.g. Martinez-Gomis *et al.*, 2009). This condition is quantitatively illustrated by the comparative cartographies of enamel thickness distribution elaborated for the postcanine teeth (Figure 4).

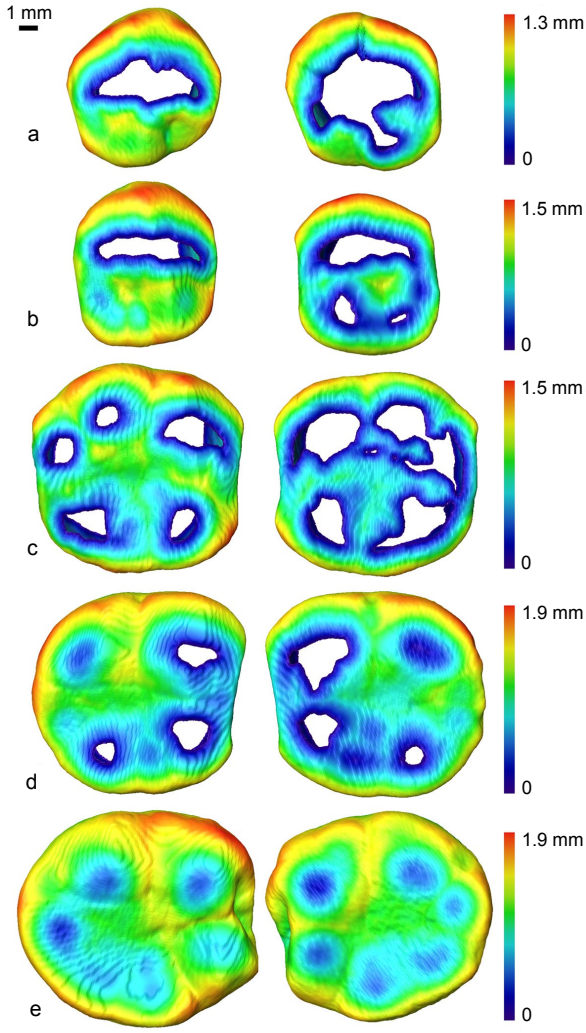

Figure 4. Comparative enamel thickness cartographies of the left (to the left) and right (to the right) lower postcanine teeth of Spy II. a: P3s; b: P4s; c: M1s; d: M2s; e: M3s. Crowns shown in occlusal view. Enamel thickness topographic variation rendered by means of a chromatic scale increasing from "thin" blue to "thick" red.

When compared to the preliminary figures from the Neandertal mandible Regourdou 1, Spy II shows a distinct, more heterogeneous antero-posterior distribution in terms of dental tissue proportions along its lower dentition (Figure 5). In particular, although it presents higher relative enamel volumes for its postcanine crowns, the individual from Betche aux Rotches also shows lower relative enamel volumes for its anterior teeth, with a particularly low value characterising its central incisors. Again, these results clearly reflect the peculiar heterogeneous wear pattern affecting the Spy II lower dentition. Here, the higher degree of occlusal wear which affects its anterior arch suggests a response to heavier mechanical constraints than those experienced by the Neandertal from Regourdou. In this regard, the lower left incisor and P4 of Spy I indicate a more homogeneous antero-posterior distribution in terms of dental tissue proportions than observed in Spy II (Table 4; see also Figure 5).

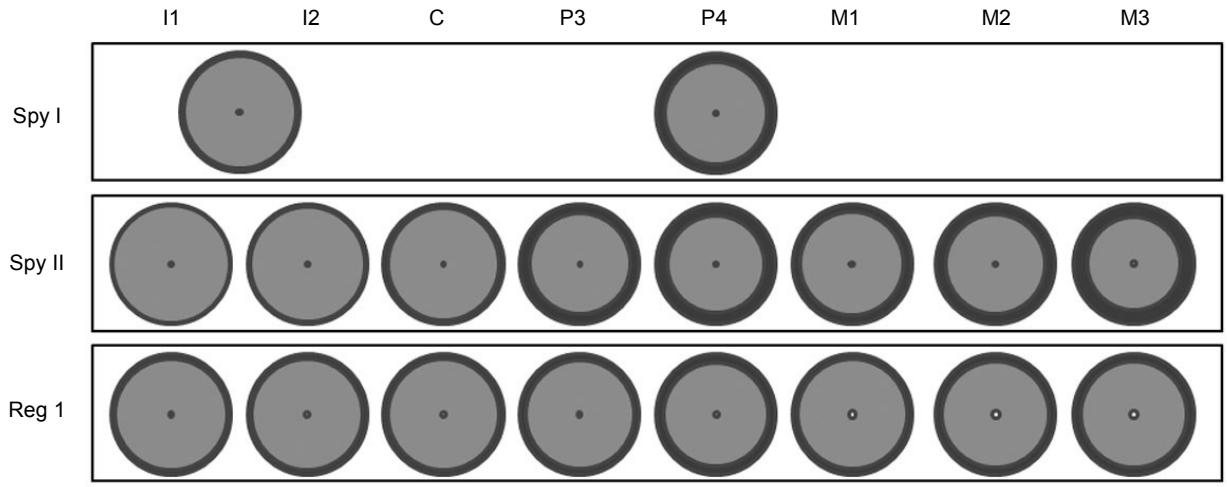

Figure 5. Relative proportions of the total tooth volume composed of enamel (in dark grey), dentine (in light grey), and pulp (in white) in the mandibular teeth of the Neandertal individuals Spy I (left teeth only; no data available for the C, P3, M1, M2, M3; uncertain position for the incisor), Spy II, and Regourdou 1 (means of left and right values).

	Enamel volume (mm^3)	*Crown dentine+ pulp volume (mm^3)*	*EDJ surface area (mm^2)*	*% of the crown volume that is dentine+pulp*	*Average Enamel Thickness (mm)*	*Relative Enamel Thickness*
UM3						
Spy I	219.16	291.13	202.19	57	1.08	16.35
Spy II	198.60	233.73	174.95	54	1.14	18.43
Neand (4)	223.44 (194.84-259.02)	339.87 (271.89-421.54)	217.28 (181.20-248.17)	60 (57.32-66.11)	1.04 (0.87-1.18)	14.97 (11.61-16.60)
EH (15)	205.50	181.65	145.10	46	1.48	26.70
LM3						
Spy II	223.45	257.39	181.01	54	1.23	19.39
Neand (8)	187.77 (140.28-261.73)	310.60 (244.62-485.90)	188.75 (142.85-228.03)	62 (56.58-68.63)	1.00 (0.78-1.30)	14.84 (12.32-19.67)
EH (10)	241.71	239.52	167.16	49	1.45	23.99

Table 5. Dental tissue proportions of the upper (UM3) and lower third molars (LM3) comparatively assessed in Spy I (no data available for the lower M3), Spy II, a Neandertal and an extant human reference sample. See text (Methods) for the description of the variables. For the UM3 of Spy I and the LM3 of Spy II, the means of the left and right estimates are reported. No data are available for the range of variation of the extant human molars.

With reference to the relatively poorly worn M3s, the results of the analysis of dental tissue proportions of Spy I (no data available for its LM3s), Spy II, and the Neandertal and extant human comparative samples are shown in Table 5.

The estimates assessed for the upper and lower M3s of Spy I and Spy II substantially fit those from the whole Neandertal sample available to us. Conversely, with respect to the modern human figures, Spy I and Spy II show similar values for the enamel volumes, but higher values for the crown dentine+pulp volume, the EDJ surface area, the percent of the crown volume that is dentine and pulp, as well as lower values for the AET and RET (Macchiarelli *et al.*, 2006; Olejniczak *et al.*, 2008; Bayle *et al.*, 2009). In this context, it should be noted that the values shown

by Spy II for the crown dentine+pulp volume, the EDJ surface area, and the percent of the crown volume that is dentine and pulp lie in the lower part of the Neandertal variation range, but that those pertaining to the average and relative enamel thickness fall within its upper portion.

CONCLUDING REMARKS

The present quantitative evidence from the microtomographic-based 3D investigation of the internal morphology of the Spy I and Spy II Neandertal dentitions fits the general patterns reported for the deciduous and permanent Neandertal teeth (Macchiarelli *et al.*, 2006, 2008; Olejniczak *et al.*, 2008; Skinner *et al.*, 2008; Bayle *et al.*, 2009). Compared to the modern human condition reported so far, both anterior and posterior Neandertal teeth are characterised by similar absolute enamel volumes, but deposited over a topographically more complex enamel-dentine junction and larger volumes of dentine, resulting in lower average and relative enamel thickness values. While some direct/ indirect relationships likely exist among these structural features typically characterising the Neandertal dentition and a number of factors, such as specific developmental mechanisms and trajectories (e.g. Suwa & Kono, 2005; Macchiarelli *et al.*, 2006; Smith *et al.*, 2007), possible metabolic rate differences (Churchill, 1998), ecological constraints or dietary specialisations (e.g. Richards *et al.*, 2001), the functional meaning and adaptive nature of these characteristics still await future research.

Some differences in dental tissue proportions have been recorded between the two contemporaneous Neandertal individuals considered in the present study, Spy I and Spy II (for the dating of the specimens, see Semal *et al.*, 2009). In such a case, sexual dimorphism (e.g. Alvesalo, 2009; Feeney, 2009) and/or inter-individual variation may be evoked among the most likely factors responsible for these quantitative differences.

Finally, when compared to the evidence from other Neandertal individuals, including Regourdou 1 and even Spy I, the mandibular dentition of Spy II shows a quite peculiar heterogeneous antero-posterior distribution in occlusal wear and tooth tissue proportions. Following the so-called "anterior dental loading hypothesis" (Brace, 1964; see also Wolpoff, 1979; Trinkaus, 1983; O'Connor *et al.*, 2005), compared to Spy I, Spy II may have been involved in more frequent and/or heavier masticatory/paramasticatory loading activities.

ACKNOWLEDGEMENTS

We would like to thank the Editors for their kind invitation to contribute to this volume and, mostly, for having put at disposition of the international scientific community the original record in their care. The *Musée d'Art et d'Archéologie du Périgord* and the *Musée d'Angoulême* kindly granted access to the comparative fossil record. For technical collaboration, we acknowledge the Micro CT Scan Research Group at the University of Antwerp (N. De Clerck), the *Centre de Microtomographie* at the University of Poitiers (P. Sardini), the ESRF beamline ID17, Grenoble (A. Bravin, C. Nemoz, and P. Tafforeau), and the NESPOS Society (www.nespos.org). Thanks also to A. Beaudet and C. Zanolli for their generous collaboration and interaction. Research supported by the Fyssen Foundation, the EU FP6 Marie Curie MRTN-CT-2005-019564 (EVAN; http://www.evan.at), and the TNT project.

BIBLIOGRAPHY

ALVESALO L., 2009. Human sex chromosomes in oral and craniofacial growth. *Archives of Oral Biology*, **54S**: S18-S24.

BAILEY S. E., 2002. A closer look at Neanderthal postcanine dental morphology: the mandibular dentition. *The Anatomical Record*, **269**: 148-156.

BAILEY S. E., SKINNER M. M. & HUBLIN J.-J., 2011. What lies beneath? An evaluation of lower molar trigonid crest patterns based on both dentine and enamel expression. *American Journal of Physical Anthropology*, **145** (4): 505-518.

BAYLE P., BRAGA J., MAZURIER A. & MACCHIARELLI R., 2009. Dental developmental pattern of the Neanderthal child from Roc de Marsal: a high-resolution 3D analysis. *Journal of Human Evolution*, **56** (1): 66-75.

BAYLE P., MACCHIARELLI R., TRINKAUS E., DUARTE C., MAZURIER A. & ZILHÃO J., 2010. Dental maturational sequences and dental tissue proportions in the early Upper Paleolithic child from Abrigo do Lagar Velho, Portugal. *Proceedings of the National Academy of Sciences USA*, **107**: 1338-1342.

BRACE C. L., 1964. The fate of “classic” Neanderthals. A consideration of hominid catastrophism. *Current Anthropology*, **5**: 3-43.

CHURCHILL S. E., 1998. Cold adaptation, heterochrony, and Neandertals. *Evolutionary Anthropology*, **7**: 46-61.

CREVECOEUR I., BAYLE P., ROUGIER H., MAUREILLE B., HIGHAM T., VAN DER PLICHT J., DE CLERCK N. & SEMAL P., 2010. The Spy VI child: a newly discovered Neandertal infant. *Journal of Human Evolution*, **59** (6): 641-656.

FEENEY R. N. M., 2009. *Microtomographic analysis of sexual dimorphism and dental tissue proportions in human molars*. Ph.D. dissertation, The Ohio State University, Columbus.

FRAIPONT J. & LOHEST M., 1886. La race humaine de Néanderthal ou de Canstadt, en Belgique. Recherches ethnologiques sur des ossements humains, découverts dans des dépôts quaternaires d'une grotte à Spy et détermination de leur âge géologique. Note préliminaire. *Bulletin de l'Académie royale des Sciences de Belgique*, 3ème série, **XII**: 741-784.

FRAIPONT J. & LOHEST M., 1887. La race humaine de Néanderthal ou de Canstadt en Belgique. Recherches ethnologiques sur des ossements humains, découverts dans des dépôts quaternaires d'une grotte à Spy et détermination de leur âge géologique. *Archives de Biologie*, **7**/1886: 587-757.

KONO R., 2004. Molar enamel thickness and distribution patterns in extant great apes and humans: new insights based on a 3-dimensional whole crown perspective. *Anthropological Science*, **112**: 121-146.

MACCHIARELLI R. & BAILEY S. E., 2007. Dental microstructure and life history: introduction. *In*: S. E. BAILEY & J.-J. HUBLIN (ed.), *Dental Perspectives on Human Evolution. State-of-the-Art Research in Dental Paleoanthropology*. Dordrecht, Springer: 139-146.

MACCHIARELLI R., BONDIOLI L., DEBÉNATH A., MAZURIER A., TOURNEPICHE J.-F., BIRCH W. & DEAN C., 2006. How Neanderthal molar teeth grew. *Nature*, **444**: 748-751.

MACCHIARELLI R., BONDIOLI L. & MAZURIER A., 2008. Virtual dentitions: touching the hidden evidence. *In*: J. D. IRISH & G. C. NELSON (ed.), *Technique and application in dental anthropology*. Cambridge, Cambridge University Press: 426-448.

MARTIN L., 1985. Significance of enamel thickness in hominoid evolution. *Nature*, **314**: 260-263.

MARTINEZ-GOMIS J., LUJAN-CLIMENT M., PALAU S., BIZAR J., SALSENCH J. & PERAIRE M., 2009. Relationship between chewing side preference and handedness and lateral asymmetry of peripheral factors. *Archives of Oral Biology*, **54**: 101-107.

O’CONNOR C. F., FRANCISCUS R. G. & HOLTON N. E., 2005. Bite force production capability and efficiency in Neandertals and modern humans. *American Journal of Physical Anthropology*, **127** (2): 129-151.

OLEJNICZAK A. J., SMITH T. M., FEENEY R. N. M., MACCHIARELLI R., MAZURIER A., BONDIOLI L., ROSAS A., FORTEA J., DE LA RASILLA M., GARCIA-TABERNERO A., RADOVČIĆ J., SKINNER M. M., TOUSSAINT M. & HUBLIN J.-J., 2008. Dental tissue proportions and enamel thickness in Neandertal and modern human molars. *Journal of Human Evolution*, **55** (1): 12-23.

RICHARDS M. P., PETTITT P. B., STINER M. C. & TRINKAUS E., 2001. Stable isotope evidence for increasing dietary breadth in the European mid-Upper Paleolithic. *Proceedings of the National Academy of Sciences USA*, **98**: 6528-6532.

ROUGIER H., CREVECOEUR I., FIERS E., HAUZEUR A., GERMONPRÉ M., MAUREILLE B. & SEMAL P., 2004. Collections de la Grotte de Spy: (re)découvertes et inventaire anthropologique. *Notae Praehistoricae*, **24**: 181-190.

SEMAL P., ROUGIER H., CREVECOEUR I., JUNGELS C., FLAS D., HAUZEUR A., MAUREILLE B., GERMONPRÉ M., BOCHERENS H., PIRSON S., CAMMAERT L., DE CLERCK N., HAMBUCKEN A., HIGHAM T., TOUSSAINT M. & VAN DER PLICHT J., 2009. New Data on the Late Neandertals: Direct Dating of the Belgian Spy Fossils. *American Journal of Physical Anthropology*, **138** (4): 421-428.

SEMAL P., TOUSSAINT M., MAUREILLE B., ROUGIER H., CREVECOEUR I., BALZEAU A., BOUCHNEB L., LOURYAN S., DE CLERCK N. & RAUSIN L., 2005. Numérisation des restes humains néandertaliens belges. Préservation patrimoniale et exploitation scientifique. *Notae Praehistoricae*, **25**: 25-38.

SKINNER M. M., WOOD B. A., BOESCH C., OLEJNICZAK A. J., ROSAS A., SMITH T. M. & HUBLIN J.-J., 2008. Dental trait expression at the enamel-dentine junction of lower molars in extant and fossil hominoids. *Journal of Human Evolution*, **54** (2): 173-186.

SMITH T. M., TOUSSAINT M., REID D. J., OLEJNICZAK A. J. & HUBLIN J.-J., 2007. Rapid dental development in a Middle Paleolithic Belgian Neanderthal. *Proceedings of the National Academy of Sciences USA*, **104**: 20220-20225.

SPOOR C. F., ZONNEVELD F. W. & MACHO G. A., 1993. Linear Measurements of cortical bone and dental enamel by computed tomography: applications and problems. *American Journal of Physical Anthropology*, **91** (4): 469-484.

SUWA G. & KONO R. T., 2005. A micro-CT based study of linear enamel thickness in the mesial cusp section of human molars: reevaluation of methodology and assessment of within-tooth, serial, and individual variation. *Anthropological Science*, **113**: 273-289.

TOUSSAINT M., OLEJNICZAK A. J., EL ZAATARI S., CATTELAIN P., FLAS D., LETOURNEUX C. & PIRSON S., 2010. The Neandertal lower right deciduous second molar from Trou de l'Abîme at Couvin, Belgium. *Journal of Human Evolution*, **58** (1): 56-67.

TRINKAUS E., 1983. *The Shanidar Neandertals*. New York, Academic Press: 502 p.

WOLPOFF M. H., 1979. The Krapina dental remains. *American Journal of Physical Anthropology*, **50** (1): 67-114.

WOOD B., 2010. Reconstructing human evolution: achievements, challenges, and opportunities. *Proceedings of the National Academy of Sciences USA*, **107**: 8902-8909.

AUTHORS AFFILIATION

Priscilla BAYLE
Université de Bordeaux
PACEA, UMR 5199
Allée Geoffroy St Hilaire
CS 50023
33615 Pessac cedex
France
p.bayle@pacea.u-bordeaux1.fr

Arnaud MAZURIER
Société Études Recherches Matériaux (E.R.M.)
CRI Biopole
86000 Poitiers
France
arnaud.mazurier@erm-poitiers.fr

Roberto MACCHIARELLI
UMR 7194
Département de Préhistoire
du Muséum national d'Histoire naturelle
43, rue Buffon
75005 Paris
France
roberto.macchiarelli@mnhn.fr
and
Département Géosciences
Université de Poitiers
rue A. Turpain, bât. B8
86022 Poitiers
France
roberto.macchiarelli@univ-poitiers.fr